Trapping of Swimming Microorganisms at Lower Surfaces by Increasing Buoyancy

Ilyong Jung,[1] Karine Guevorkian,[2] and James M. Valles[1,*]
[1]Department of Physics, Brown University, Providence, Rhode Island 02912, USA
[2]Institut de Génétique et de Biologie Moléculaire et Cellulaire (IGBMC), CNRS (UMR 7104), Inserm U964, Université de Strasbourg, Illkirch F-67400, France
(Received 28 April 2014; published 17 November 2014)

Models suggest that mechanical interactions alone can trap swimming microorganisms at surfaces. Testing them requires a method for varying the mechanical interactions. We tuned contact forces between *Paramecia* and surfaces *in situ* by varying their buoyancy with nonuniform magnetic fields. Remarkably, increasing their buoyancy can lead to ~100% trapping at lower surfaces. A model of *Paramecia* in surface contact passively responding to external torques quantitatively accounts for the data implying that interactions with a planar surface do not engage their mechanosensing network and illuminating how their trapping differs from other smaller microorganisms.

DOI: 10.1103/PhysRevLett.113.218101 PACS numbers: 47.63.Gd, 87.17.Jj, 87.17.Rt, 87.18.Gh

Swimming organisms interact with surfaces as they negotiate their environs [1–5]. Higher organisms, such as fish, use whiskers, eyes, and other means to detect obstacles that they actively avoid by adjusting their swimming. Lower organisms appear to navigate around obstacles much more passively [6–10]. Studies of bacteria, for example, indicate that hydrodynamic and contact interactions between swimmers and surfaces drive them to passively accumulate [2,10]. That is, the interactions closely related with collective bacterial behavior such as biofilm formation [11] and swarming [12] do not appear to lead to a change in the propulsion that could be considered an active response. Here we present investigations of surface interactions for another swimming unicellular organism, *Paramecium*, which is known to actively respond to mechanical perturbations [13]. When prodded in the posterior they accelerate away and when prodded in the anterior they perform an avoiding reaction, backing up to swivel off in a new swimming direction [14,15]. We address whether their collisions with nearly planar surfaces evoke similar active changes in propulsion.

Paramecia are among the many microorganisms small enough that their motion occurs at low Reynolds number (Re) but large enough that their apparent weight, $\vec{w}$, influences their swimming [16–26]. This combination indicates that surface collision forces might be large enough to provoke an active response. We demonstrate this by first estimating the scale of the collision forces. A freely swimming *Paramecium* experiences forces that decompose typically into propulsion, P, and drag, D. These sum to zero at low Re [27,28]. At the moment of a head-on collision, the drag force drops out and the normal force, N, exerted by the surface grows to balance P. Consequently, the propulsive force sets the collision force scale. In the presence of gravity, *Paramecia* must swim hard enough that $P > w$ in order for them to stay suspended. Altogether, the collision force is expected to exceed the apparent weight force.

The influence of the apparent weight force on *Paramecia* swimming has been categorized into two phenomena. They show negative gravitaxis which is a tendency to orient their swimming direction antiparallel to the gravity vector [29–31]. They also exhibit negative gravikinesis by exerting a stronger propulsive force when swimming against their apparent weight [32–34]. Both behaviors disappear when *Paramecia* are neutrally buoyant [30,35]. The gravitactic response appears to be a passive response to a mechanical torque arising from an asymmetry of the *Paramecium* body [29]. The gravikinetic response, on the other hand, appears to be active. How *Paramecia* transduce the very small apparent weight force (~100 pN) remains unclear [14,31,32,35]. The main proposal attributes it to the mechanical activation of ion channels which changes the membrane potential and consequently ciliary beating [36]. Thus, *Paramecia* are suspected of actively responding to a force that is smaller than forces involved in collisions.

Here, we show that applying forces and torques comparable to the propulsive force influence *Paramecium*'s interactions with upper and lower surfaces. We were motivated by unexpected observations of two species of *Paramecia* becoming trapped at lower surfaces when they were buoyant. We used a magnet based technique, magnetic force buoyancy variation, for adjusting $\vec{w}$ *in situ* [35]. The magnetic field employed also exerted a torque that aligned *Paramecia* to swim along the vertical magnetic field lines. The torque arises from an intrinsic magnetic susceptibility anisotropy, $\Delta\chi = (\chi_{\parallel} - \chi_{\perp})$, where $\chi_{\parallel}$ and $\chi_{\perp}$ are the susceptibilities parallel to and perpendicular to a *Paramecium* long axis. We observe that these imposed forces and torques control the surface trapping by enhancing or inhibiting the turning of *Paramecia* that allows them to escape from surfaces. We present a passive mechanical

model that quantitatively accounts for the range of observed phenomena. In particular, it explains the counterintuitive result that forces directed away from a surface drive trapping at the surface. The two species of *Paramecia* behave slightly differently from one another in a manner that can be captured by adjusting $\Delta\chi$, $\vec{w}$, and P.

We applied magnetic force buoyancy variation by placing swimming chambers in the bore of a high field resistive magnet at the National High Magnetic Field Laboratory [37]. Adjusting the magnet current and/or chamber position varies the magnetic force acting on the *Paramecia* and the solution to alter the apparent weight of the *Paramecia*. We can specify the magnetically modified apparent weight, w as

$$\frac{w}{w_{1g}} = 1 \pm \left(\frac{B}{B_{\text{neut}}}\right)^2 \quad (1)$$

where B, w_{1g}, and B_{neut} are the magnetic field, the apparent weight at $1g$, and the magnetic field at neutral buoyancy, respectively. The $-$ and $+$ signs are for positions above and below the magnet center. B_{neut}, which was 10 T for *P. tetraurelia* and 7.8 T for *P. caudatum*, is the field at which immobilized *Paramecia* ceased to sediment. (See the Supplemental Material [38] for more experimental details.)

Paramecia tetraurelia (P. tetraurelia) (120–150 μm long) tended to become trapped at surfaces when $\vec{w}$ was directed away from the surface [Fig. 1(a)]. Individual swimmers in movie, Supplemental Material [38], M-1 swam into a surface at a speed constant to within a few percent, rotated toward parallel, and then swam canted at a constant angle along the surface at a constant speed with their anterior in contact. Some swam in circles that were usually left handed like the helices of free swimmers. *Paramecia* escaped the surface generally after colliding with another *Paramecium*, a dust particle, or the chamber walls. Rotational diffusion effects known to influence bacteria surface escape [6] were not apparent as expected for these much larger organisms. Occasionally *P. tetraurelia* assumed a static vertical orientation. By contrast, the *P. tetraurelia* that swam toward the surface with $\vec{w}$ only briefly made contact as they reversed their swimming direction (See Supplemental Material [38], M-2).

We used a surface trapping probability (STP) to capture the dependence of the trapping on w/w_{1g} [Figs. 1(b) and 1(c)]. The STP is the fraction of the swimmers colliding with a surface that subsequently reside on it for a time necessary to swim many body lengths. We chose 3 s. We observed 20 collisions for each data point and measured the STP every 30 seconds. The STP increases from near zero at $w/w_{1g} = 1$ to about 80% at $w/w_{1g} = -2$. This correlation is strong evidence that $\vec{w}$ controls the trapping.

Paramecium caudatum (P. caudatum) (180–250 μm long) also showed $\vec{w}$ dependent surface trapping. Like *P. tetraurelia*, they approached the surface, made an incomplete turn toward parallel, and swam along it at a

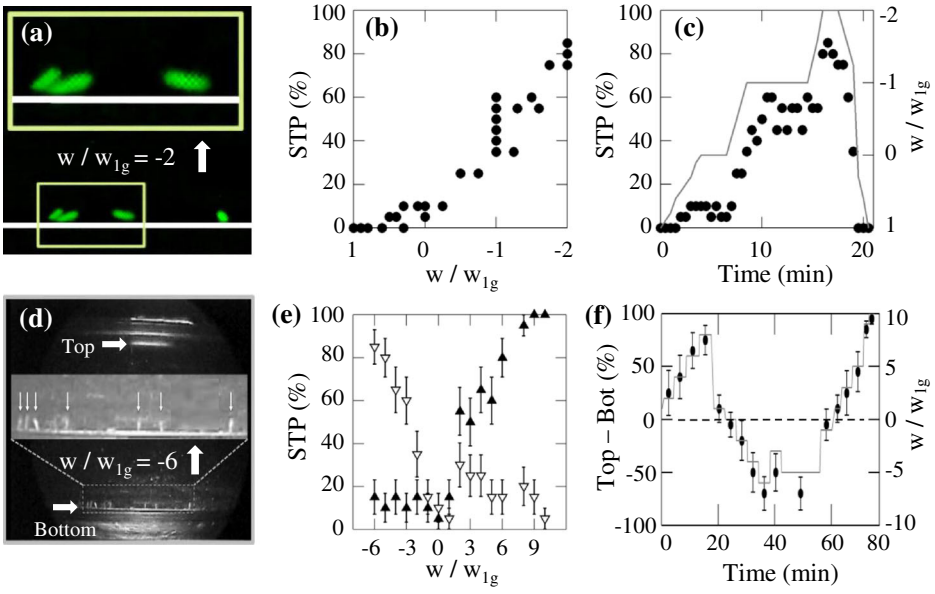

FIG. 1 (color online). (a) The surface trapping probability (STP) of *P. tetraurelia* at the bottom. Frame showing 3 *P. tetraurelia* at the bottom surface when $w/w_{1g} = -2$. The long axes of their bodies were canted away from horizontal as they swam along the surface. (b) STP of *P. tetraurelia* near the bottom surface as w/w_{1g} changes from 1 to -2. The negative force indicates that the force direction is from the bottom to the top. (c) STP of *P. tetraurelia* and w/w_{1g} (solid line) as a function of time. w was changed in steps. (d) Trapping of *P. caudatum* at the bottom surface. Upward apparent weight force ($w/w_{1g} = -6$) is applied. (e) STP of *P. caudatum* at the top (triangle) and bottom (downward triangle) surface. (f) STP of *P. caudatum* at the top surface minus the bottom surface and w/w_{1g} as a function of time. The solid line marks the changes in w/w_{1g}. The dotted line denotes where both the probability and w/w_{1g} are zero. The bars on the points give the uncertainty estimated presuming the measurements followed a binomial distribution.

constant speed and canting angle. Their escape appeared to be dictated by collisions. Trapped *P. caudatum* were usually oriented vertically [Fig. 1(d) and Supplemental Material [38] M-3] while a few, usually at lower apparent weights, swam canted relative to the surface (See Supplemental Material [38], M-4). Vertically oriented *P. caudatum* often swayed about 15 degrees with a period of about 1 s.

Figure 1(e) shows the STP for *P. caudatum* on both the top and bottom surfaces as w/w_{1g} varies from -6 to 10. Very little trapping occurred for $-2 \le w/w_{1g} \le 2$. At the most negative apparent weights, the bottom STP approached 100% and the top STP remained low. At the most positive apparent weights these behaviors exchanged (See Supplemental Material [38], M-5). The difference between the top and bottom STPs closely tracks the changes in w/w_{1g} [Fig. 1(f)]. The videos indicate that when the STP on either surface is low the *P. caudatum* easily turned at the surface to swim away (See Supplemental Material [38], M-5). Thus, like *P. tetraurelia*, trapping occurred primarily for *P. caudatum* swimming against $\vec{w}$ on their way to a surface.

In addition, *P. caudatum* became trapped by intense homogeneous magnetic fields for which $w/w_{1g} = 1$. Figure 2 shows that the STPs for both the top and bottom surfaces grow with the magnetic field. The top STP is slightly higher at each field. The trapped *P. caudatum* were primarily vertical on both surfaces.

The strong w and B dependence of the STP led us to consider a model of mechanical torques that contribute to turning at surfaces. The model [Fig. 3(a)] presumes a passive swimmer with a prolate ellipsoid shaped body with major axis, L, that swims in a plane and approaches the surface at normal incidence. It ignores the helical motion, which causes it to wobble as a first approximation. The body interacts with the surface through a normal force $\vec{N}$. $\vec{w}$, $\vec{D}$, and $\vec{P}$, which is oriented along the long axis, act at the center. P is presumed constant since *Paramecia* approach and swim along the surfaces at constant speeds. Correspondingly, the model neglects stochastic variations in the propulsive mechanism, which can influence smaller organisms [6]. Also, it neglects long-range hydrodynamic interaction between *Paramecia* as phenomena like dancing *Volvox* [39] were not apparent. At low Re number, $\vec{P} + \vec{N} + \vec{D} + \vec{w} = 0$. The perpendicular components satisfy $N = P\cos\theta - \vec{w}\cdot\hat{n}$ where θ is the angle between the long axis and the surface normal, $\hat{n}$.

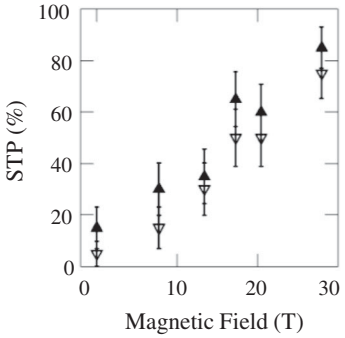

FIG. 2. STP at the top (triangle) and bottom (downward triangle) surface as a function of homogeneous magnetic field at constant apparent weight of $w/w_{1g} = 1$. The bars on the points give the uncertainty estimated presuming the measurements followed a binomial distribution.

The torques turning the body about its center also sum to zero, $\vec{\tau}_N + \vec{\tau}_B + \vec{\tau}_D = 0$, where

$$\tau_N = \frac{L}{2} N \sin\theta = \frac{L}{2}(P\cos\theta - \vec{w}\cdot\hat{n})\sin\theta \qquad (2)$$

is the normal force torque,

$$\tau_B = -\frac{1}{2\mu_0}\Delta\chi B^2 \sin 2\theta \qquad (3)$$

is the magnetic torque, and τ_D is the drag torque. μ_0 is the permeability of free space. Because $\Delta\chi > 0$, τ_B aligns *Paramecia* to swim along the magnetic field. $\Delta\chi$ is large enough to orient the vast majority of *Paramecia* essentially to swim vertically in magnetic fields as low as 3 T [40].

It is noteworthy that this model leaves out a hydrodynamic force dipole image torque that appears to align

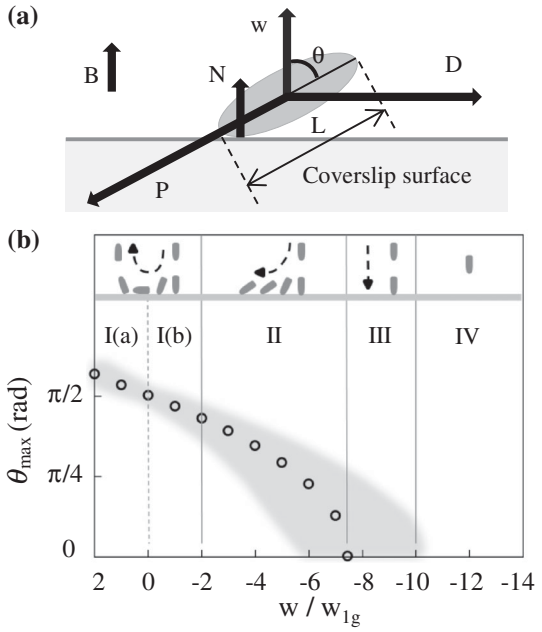

FIG. 3. (a) A sketch of a canted *Paramecium* in contact with and swimming along the bottom surface. In this figure, the *Paramecium* swims against $\vec{w}$. (b) Phase diagram of *P. caudatum* behavior at the bottom surface. The upper four frames give schematics of the swimming behavior in the magnetic field regions I–IV. The gray region specifies the range of $\theta_{\max}$ expected for a typical population of swimmers.

bacteria parallel to surfaces to trap them [6] and the gravitactic torque [29]. If the dipole torque played a role, then *Paramecia* that turned to parallel would stay trapped, which is contrary to the observations. A plausible explanation for this different behavior is that the force dipole, Pl, is relatively smaller for *Paramecia* than for bacteria. Here l is the distance between the center of drag and propulsion. For bacteria like *Escherichia coli* (*E. coli*), $l \approx L$ since the center of drag is near the body center and the center of propulsion is near the center of the flagellar bundle. Consequently, the torque due to propulsion, which scales as PL is comparable to the dipole torque for *E. coli*. For *Paramecia*, however, $Pl \ll PL$, as the propulsion involves the beating of cilia that uniformly cover the body, which makes the centers of drag and propulsion nearly coincide. Thus, it is reasonable to omit this hydrodynamic dipole image torque. The gravitactic torque, which can be written as wc where c is a body asymmetry length, is estimated to be less than 5% of wL which makes its contribution to turning at a surface negligible.

We define the torque that drives turning as $\tau_{\text{drive}} = \tau_N + \tau_B$. When $\tau_{\text{drive}} > 0$, the long axis of a *Paramecium* rotates toward parallel to the surface. τ_D simply opposes this motion. Swimmers rotate up to a maximum angle $\theta_{\max}$, where $\tau_{\text{drive}}(\theta_{\max}) = 0$:

$$\theta_{\max} = \cos^{-1}\left(\frac{\vec{w}\cdot\hat{n}}{P - \frac{2}{\mu_0 L}\Delta\chi B^2}\right). \tag{4}$$

They swim along the surface canted at $\theta_{\max}$.

This model predicts four distinct behaviors as a function of w/w_{1g}. They are depicted for a lower surface in Fig. 3(b) with a plot of $\theta_{\max}$ appropriate for *P. caudatum* (see below). At the most positive w/w_{1g}, regions I(a) and I(b), τ_{drive} rotates the swimmers to $\theta_{\max} \gtrsim \pi/2$. Because their helical motion causes them to wobble by an angle $\theta_w \approx 15°$, we presume that swimmers rotated by more than $\pi/2 - \theta_w$ are able to wobble their way through a complete turn. In region II, where $\pi/2 - \theta_w > \theta_{\max} > 0$, τ_{drive} rotates them to swim at a canted angle $\theta_{\max}$. In region III, the magnetic torque dominates to prevent the rotation of the swimmers to leave them vertical. Finally, in region IV, the force stalls the swimmers before they reach the surface. These behaviors are evident in the videos.

The model also quantitatively accounts for the data. The points in Fig. 3(b) were plotted using

$$\theta_{\max} = \cos^{-1}\left(\frac{-w/w_{1g}}{\frac{P}{w_{1g}} \pm \frac{2\Delta\chi B_{\text{neut}}^2}{\mu_0 w_{1g} L}(1 - w/w_{1g})}\right), \tag{5}$$

where the plus and minus signs are for *Paramecia* swimming into the bottom surface along and against forces, respectively. Note that the positive direction of w is defined as the normal gravity direction. The measured average parameters P, w_{1g}, $\Delta\chi$, B_{neut}, μ_0, and L for *P. caudatum* are 1000 pN, 100 pN, 6.7×10^{-23} m^3 [40], 7.8 T, $4\pi \times 10^{-7}$ H m^{-1}, and 215 μm, respectively. Thus the model predicts that average *Paramecia* turn successfully for $w/w_{1g} > -2$, become trapped for $w/w_{1g} < -2$, and become vertically oriented at $w/w_{1g} \simeq -7.5$ in accord with Fig. 1(e) and the video observations. The range of behaviors exhibited at a fixed value of w/w_{1g} can be attributed to the variation in P, w_{1g}, and $\Delta\chi$ in the population. The gray band in Fig. 3(b) is the expected spread in $\theta_{\max}$ if we presume that P varies by $\pm 25\%$ [41]. This band implies, for example, that when $w/w_{1g} \simeq -7.5$, some trapped swimmers are predicted to be canted while others are oriented normal.

While *P. tetraurelia* and *P. caudatum* behave very similarly, the model predicts differences that are observed. *P. tetraurelia* has a smaller ratio of w_{1g}/P, which reduces the field scale over which trapping is observed (Fig. 1). In addition, *P. tetraurelia* is a factor of 2 shorter than *P. caudatum* which leads to a weaker magnetic susceptibility anisotropy [40] and less of a tendency for them to orient vertically while trapped at a surface.

Overall, this passive model appears to capture the magnetic force buoyancy variation driven trapping phenomena. This passive response to surface interactions agrees with smaller microorganism behavior. The surface accumulation of *E. coli* [4] and *Caulobacter Crescentus* [2] and the surface guiding of other microorganisms that has been exploited to create ratchets [7,8] do not appear to involve changes in propulsive output [9,10].

Closer inspection of *Paramecia* swimming into surfaces with higher spatial and temporal resolution than employed here is required to eliminate the contribution of active responses. There are some indications that the *Paramecia* swimming with the apparent weight into surfaces bounce on impact at the highest w/w_{1g}. This effect might be a slight avoiding reaction and thus a sign of an active response. The results presented here, however, imply that *Paramecium* navigation around smooth obstacles is dominated by simple mechanics involving short-range forces.

We are grateful for discussions with Jay Tang. We also thank Michael Wagman and Harry Mickalide for making helpful contributions to the experiments. This work was supported by NSF Grant No. PHY0750360 and at the National High Magnetic Field Laboratory by NSF Grant No. DMR-0084173. This work was also supported by National Aeronautics and Space Administration Grant No. NAG3-2882.

*valles@brown.edu

[1] S. Jana, S. H. Um, and S. Jung, Phys. Fluids **24**, 041901 (2012).
[2] G. Li and J. X. Tang, Phys. Rev. Lett. **103**, 078101 (2009).
[3] G. Li, J. Bensson, L. Nisimova, D. Munger, P. Mahautmr, J. X. Tang, M. R. Maxey, and Y. V. Brun, Phys. Rev. E **84**, 041932 (2011).

[4] A. P. Berke, L. Turner, H. C. Berg, and E. Lauga, Phys. Rev. Lett. **101**, 038102 (2008).
[5] I. Tuval, L. Cisneros, C. Dombrowski, C. W. Wolgemuth, J. O. Kessler, and R. E. Goldstein, Proc. Natl. Acad. Sci. U.S.A. **102**, 2277 (2005).
[6] K. Drescher, J. Dunkel, L. H. Cisneros, S. Ganguly, and R. E. Goldstein, Proc. Natl. Acad. Sci. U.S.A. **108**, 10 940 (2011).
[7] P. Galajda, J. Keymer, P. Chaikin, and R. H. Austin, J. Bacteriol. **189**, 8704 (2007).
[8] G. Lambert, D. Liao, and R. H. Austin, Phys. Rev. Lett. **104**, 168102 (2010).
[9] P. Denissenko, V. Kantsler, D. J. Smith, and J. Kirkman-Brown, Proc. Natl. Acad. Sci. U.S.A. **109**, 8007 (2012).
[10] V. Kantsler, J. Dunkel, M. Polin, and R. E. Goldstein, Proc. Natl. Acad. Sci. U.S.A. **110**, 1187 (2013).
[11] L. A. Pratt and R. Kolter, Mol. Microbiol. **30**, 285 (1998).
[12] M. F. Copeland and D. B. Weibel, Soft Matter **5**, 1174 (2009).
[13] R. Bräucker, R. S. Machemer, and H. Machemer, J. Exp. Biol. **197**, 271 (1994).
[14] M. Gebauer, D. Watzke, and H. Machemer, Naturwissenschaften **86**, 352 (1999).
[15] H. S. Jennings, *Behavior of the Lower Organisms* (Columbia University Press, New York, 1906).
[16] A. M. Roberts, Biol. Bull. **210**, 78 (2006).
[17] T. Fenchel and B. J. Finlay, J. Exp. Biol. **110**, 17 (1984).
[18] I. Block, N. Freiberger, O. Gavrilova, and R. Hemmersbach, Adv. Space Res. **24**, 877 (1999).
[19] R. Hemmersbach, R. Voormanns, W. Briegleb, N. Rieder, and D.-P. Häder, J. Biotechnol. **47**, 271 (1996).
[20] R. Bräucker, S. Machemer-Röhnisch, H. Machemer, and A. Murakami, European Journal of protistology **28**, 238 (1992).
[21] H. Winet and T. L. Jahn, J. Theor. Biol. **46**, 449 (1974).
[22] D. A. Noever, R. Cronise, and H. C. Matsos, Biophys. J. **67**, 2090 (1994).
[23] U. Kowalewski, R. Braucker, and H. Machemer, Microgravity Sci. Technol. **11**, 167 (1998).
[24] B. Eggersdorfer and D. P. Häder, FEMS Microbiol. Lett. **85**, 319 (1991).
[25] D. P. Häder, A. Rosum, J. Schäfer, and R. Hemmersbach, J. Biotechnol. **47**, 261 (1996).
[26] D. P. Häder, R. Hemmersbach, and M. Lebert, *Gravity and the Behavior of Unicellular Organisms* (Cambridge University Press, Cambridge, England, 2005).
[27] E. M. Purcell, Am. J. Phys. **45**, 3 (1977).
[28] E. Lauga and T. R. Powers, Rep. Prog. Phys. **72**, 096601 (2009).
[29] A. M. Roberts, J. Exp. Biol. **213**, 4158 (2010).
[30] R. Hemmersback, R. Voormanns, and D. P. Hader, J. Exp. Biol. **199**, 2199 (1996).
[31] R. Bräucker *et al.*, J. Exp. Biol. **201**, 2103 (1998).
[32] H. Machemer, R. S. Machemer, R. Bräucker, and K. Takahashi, J. Comp. Physiol. A **168**, 1 (1991).
[33] S. A. Baba, Y. Moagmi, and T. Otsu, Adv. Space Res. **23**, 2065 (1999).
[34] M. Ooya, Y. Mogami, A. Izumikurotani, and S. A. Baba, J. Exp. Biol. **163**, 153 (1992).
[35] K. Guevorkian and J. M. Valles, Proc. Natl. Acad. Sci. U.S.A. **103**, 13 051 (2006).
[36] H. Machemer, J. Exp. Biol. **65**, 427 (1976).
[37] K. Guevorkian and J. M. Valles, Rev. Sci. Instrum. **76**, 103706 (2005).
[38] See Supplemental Material at http://link.aps.org/supplemental/10.1103/PhysRevLett.113.218101 for movies depicting phenomena and additional experimental details.
[39] K. Drescher, K. Leptos, I. Tuval, T. Ishikawa, T. Pedley, and R. Goldstein, Phys. Rev. Lett. **102**, 168101 (2009).
[40] K. Guevorkian and J. M. Valles, Biophys. J. **90**, 3004 (2006).
[41] I. Jung, T. R. Powers, and J. M. Valles, Biophys. J. **106**, 106 (2014).